

Regular and Chaotic Motions of a Chaplygin Sleigh under Periodic Pulsed Torque Impacts

Alexey V. Borisov^{1,2*} and Sergey P. Kuznetsov^{1**}

¹*Udmurt State University,
ul. Universitetskaya 1, Izhevsk, 426034 Russia*

²*Moscow Institute of Physics and Technology,
Institutskii per. 9, Dolgoprudnyi, 141700 Russia*

Received October 26, 2016; accepted December 05, 2016

Abstract—For a Chaplygin sleigh on a plane, which is a paradigmatic system of nonholonomic mechanics, we consider dynamics driven by periodic pulses of supplied torque depending on the instant spatial orientation of the sleigh. Additionally, we assume that a weak viscous force and moment affect the sleigh in time intervals between the pulses to provide sustained modes of the motion associated with attractors in the reduced three-dimensional phase space (velocity, angular velocity, rotation angle). The developed discrete version of the problem of the Chaplygin sleigh is an analog of the classical Chirikov map appropriate for the nonholonomic situation. We demonstrate numerically, discuss and classify dynamical regimes depending on the parameters, including regular motions and diffusive-like random walks associated, respectively, with regular and chaotic attractors in the reduced momentum dynamical equations.

MSC2010 numbers: 37J60, 37C10, 34D45, 37E30, 34C60

DOI: 10.1134/S1560354716070029

Keywords: Chaplygin sleigh, nonholonomic mechanics, attractor, chaos, bifurcation

1. INTRODUCTION

The study of complex dynamics of nonlinear systems, including dynamical chaos, is one of the fundamental interdisciplinary problems. To date, a vast amount of material has been accumulated, including a large body of theoretical results, methodologies and algorithms, examples of model systems with complex dynamics, experimental data, and so forth [1–3]. Great interest is being expressed in applications of concepts of nonlinear dynamics [4, 5], in particular, with regard to systems of mechanical nature [6].

As is well known, constraints in mechanical systems are classified into holonomic and nonholonomic, or integrable and nonintegrable [7–9].

Consideration of the holonomic constraints defined by the relations for the generalized coordinates leaves us in the framework of the Hamiltonian formalism. Nonintegrable constraints, on the other hand, are defined by relations not only for the coordinates, but also for the generalized velocities (in which they are usually linear), and cannot be reduced to integrable ones. For a discussion of integrability criteria and the formal apparatus of nonholonomic mechanics, see the recent review [10]. In contrast to Hamiltonian mechanics, nonholonomic systems have much more various behaviors depending on the parameters; this feature has been named in [11] as hierarchy of dynamics. Nonholonomic mechanics contains many problems which are of great practical importance and are mainly related to systems associated with rolling: dynamics of wheeled vehicles, spherical robots, etc. Discrete nonholonomic systems occur in simulations of bipedal walking [12].

*E-mail: borisov@rcd.ru

**E-mail: spkuz@yandex.ru

The history of the study of nonholonomic systems is rich in dramatic events, including errors made by prominent researchers and corrected only afterwards in the course of further careful analysis [10].

Nonholonomic systems hold a special place in dynamical systems theory [9, 11]. Even in the absence of friction, under conditions of conservation of mechanical energy, they can exhibit behaviors characteristic of dissipative rather than conservative dynamics, when attractors occur on an energy surface in the phase space, like stable equilibrium states, limit cycles, or strange attractors [11, 13–17]. This is possible because, generally, the Liouville theorem is not applicable, and the phase volume in the course of evolution in time may undergo compression or expansion in some domains of the phase space. Respectively, attractors or repellers can be located in those domains.

In view of the enormous diversity of phenomena in dynamical systems, it is extremely important to undertake efforts to understand and classify them in a specific context of nonholonomic mechanical systems.

A paradigmatic example of nonholonomic mechanics is the model of Chaplygin sleigh [18–20]. This is a rigid body which can move with three legs in contact with the surface: two of them slide without friction, and the third is a knife edge attached to the sleigh and able only to slide in the longitudinal direction.

The aim of this paper is to expose and explore dynamical phenomena which occur during motion of the Chaplygin sleigh under the action of a periodic sequence of pulses of torque. We will analyze the dynamics in the presence of weak viscous friction that slows down the movement of the sleigh during the time interval between the pulses. Such a formulation of the problem is motivated, firstly, by the fact that it is interesting to compare the results with the known dynamical phenomena relating to dissipative systems [21, 22] exhibiting some features associated with the nonholonomic mechanical nature of the object. Secondly, there are some curious prospects of controlling the motion by changing the intensity of pulses or other parameters using chaos control methods [23–25] for purposeful displacements of the sleigh, particularly in the situation of diffusion-type movements observed at high intensity of pulses. This may be of interest in the context of problems of robotics, including the case of micro-objects such as those mentioned in Ref. [26].

2. BASIC EQUATIONS

Consider a Chaplygin sleigh on a flat surface. We use a laboratory reference frame (X, Y) and a frame attached to the sleigh (ξ, η) , with origin at the point of the knife edge location A (Fig. 1). The condition of the nonholonomic mechanical constraint is that the direction of velocity for point A is fixed relative to the sleigh. This can be interpreted by imagining that the knife edge is attached to the sleigh at point A , and it may slide in the direction of the knife edge, while motions across the knife edge are prohibited. We assume that the direction of the knife edge is along the axis ξ of the coordinate frame attached to the sleigh, and the center of mass C is located on the same axis at distance a from the knife edge. The reaction force, which prevents transverse motions of the knife edge is perpendicular to it and directed along the η axis.

Suppose that the torque M and the force F are applied, which will be considered relative to the position of the knife edge. It is natural in this case to take into account only the force component along ξ in the frame attached to the sleigh (the reaction force will compensate for the transversal component even if it exists).

The equations of motion are

$$\begin{aligned} m\dot{u}_A &= m\omega^2 + F, \\ (J + ma^2)\dot{\omega} &= -m\omega u_A + M, \\ \dot{\varphi} &= \omega, \\ \dot{X}_A &= u_A \cos \varphi, \quad \dot{Y}_A = u_A \sin \varphi. \end{aligned}$$

Here, m is the mass of the sleigh, J is the moment of inertia, φ is the angle of rotation of the sleigh axis relative to the laboratory frame, u_A is the velocity of the knife edge A , ω is the angular velocity of the sleigh, and X_A and Y_A are the coordinates of the knife edge in the laboratory frame.

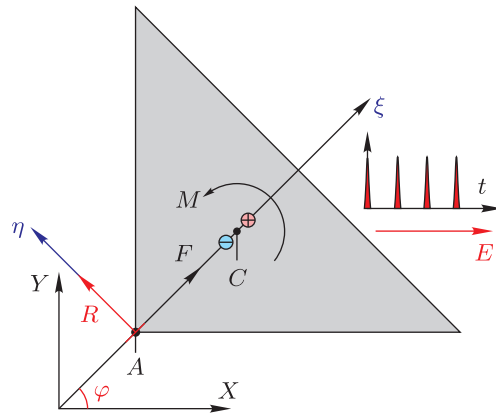


Fig. 1. Chaplygin sleigh under the action of force F and torque M . The knife edge attached at point A is oriented as shown by the red segment. The center of mass C is located at distance a from the knife edge on the axis ξ . The laboratory reference frame (X, Y) and the frame fixed relatively to the sleigh (ξ, η) are used.

The nontrivial dynamics worth studying occurs if the impulse driving is carried out with periodic kicks of applied torque M . One can imagine, say, that an electric dipole is attached to the sleigh, and the motion occurs in the presence of periodic pulses of a uniform electric field switched on and off, so that $M_p = P \sin \varphi \sum \delta(t - n\bar{T})$. In addition, we assume the presence of a weak viscous friction contributing both to the force and torque acting on the sleigh, $F_f = -\gamma u_A$ and $M_f = -\gamma_0 \omega$, respectively.

Under these assumptions the equations read

$$\begin{aligned} m\dot{u}_A &= ma\omega^2 - \gamma u_A, \\ (J + ma^2)\dot{\omega} &= -ma\omega u_A - \gamma_0 \omega + P \sin \varphi \sum \delta(t - n\bar{T}), \\ \dot{\varphi} &= \omega, \\ \dot{X}_A &= u_A \cos \varphi, \quad \dot{Y}_A = u_A \sin \varphi. \end{aligned}$$

To transform them to the dimensionless form, we use a change of variables and parameters: $u_A = uak$, $t = \tau/k$, $\omega = k\Omega$, $\mu = J/ma^2 + 1$, $\alpha = \gamma/km$, $\alpha_0 = \gamma_0/kma^2$, $k = P/ma^2$, $T = \bar{T}k$, $k = P/ma^2$, $X_A = Xa$, $Y_A = Ya$. Taking into account that the δ -function is normalized by the rule $\delta(\tau/k) = k\delta(\tau)$, we have

$$\begin{aligned} \dot{u} &= \Omega^2 - \alpha u, \\ \mu\dot{\Omega} &= -\Omega u - \alpha_0 \Omega + \sin \varphi \sum \delta(\tau - nT), \\ \dot{\varphi} &= \Omega, \\ \dot{X} &= u \cos \varphi, \quad \dot{Y} = u \sin \varphi, \end{aligned} \tag{2.1}$$

where the dot means now the derivative with respect to dimensionless time τ .

As can be seen, the first three equations for the velocity, angular velocity, and the rotational angle separate, and we may analyze them regardless of the last two equations. This set of three equations will be called *the reduced system*, and we will refer the space of variables (u, Ω, φ) as *the reduced phase space*.

Immediately after each kick, the sleigh gets a torque and, accordingly, acquires a certain angular velocity, whose value depends on the instant orientation of the sleigh. Because of the constraint, it begins to slide with rotation to keep the velocity of the reference point A in the direction along the knife edge; the angular velocity decreases, while the directed velocity grows, tending to maximum. At this short-time stage, the nonholonomic nature of motion reveals itself, while friction and mechanical energy loss may be thought negligible. At the next, long-time stage, the energy decreases gradually due to viscous friction. To the end, the rotational motion practically stops, although slow translational residual motion occurs yet in the direction of the knife edge. Its

orientation in the laboratory frame determines the value of torque, which the sleigh will take under the effect of the next kick.

The general character of the motion depends surely on the parameter of intensity of the kicks. For very small values of k the result will obviously be a stop of the sleigh with the knife edge orientation parallel to the external field. An increase in k , as we shall see, gives rise initially to periodic and then to irregular modes of motion. It turns out that the threshold of the complex dynamics in k decreases with the growing parameter $\mu = J/ma^2 + 1$, which takes into account the moment of inertia of the sleigh.

The spectrum of Lyapunov exponents of the system (2.1) contains two trivial zero exponents associated with shifts in the plane along the X and Y coordinates, and three nontrivial exponents related to the reduced system. In the presence of a positive exponent, the dynamics will be chaotic.

3. ANALYTICAL EXAMINATION: INTEGRABLE CASE

Consider a special case when the coefficients of viscous friction for translational and rotational motions have values that provide the same damping rate of these motions, namely, $\alpha_0 = \mu\alpha$. Then the set of equations for the velocity, angular velocity, and the rotation angle takes the form

$$\begin{aligned} \dot{u} + \alpha u &= \Omega^2, \\ \mu(\dot{\Omega} + \alpha\Omega) &= -\Omega u + k \sin \varphi \sum \delta(\tau - nT), \\ \dot{\varphi} &= \Omega, \end{aligned} \quad (3.1)$$

and one can derive analytically a map describing the transformation of the set of variables (u, Ω, φ) over a period of kicks.

Suppose that at time $\tau = nT - 0$ the dimensionless velocity is u_n , the angular velocity is Ω_n , and the orientation of the sleigh is determined by the angle φ_n . Then, after the kick, the initial conditions for the variables u and Ω are

$$u = u_n, \quad \Omega = \Omega_n + k\mu^{-1} \sin \varphi_n,$$

and on the time interval until the next kick we have to solve the equations

$$\dot{u} + \alpha u = \Omega^2, \quad \mu(\dot{\Omega} + \alpha\Omega) = -\Omega u.$$

Upon the substitution

$$u = Ue^{-\alpha t}, \quad \Omega = We^{-\alpha t},$$

where t is dimensionless time measured from the moment of the kick, we have

$$\dot{U} = W^2 e^{-\alpha t}, \quad \mu \dot{W} = -WU e^{-\alpha t}.$$

This implies

$$U^2 + \mu W^2 = \text{const},$$

and it makes sense to seek a solution in the form

$$U = R \cos \Phi, \quad W = R\mu^{-\frac{1}{2}} \sin \Phi,$$

where $R = \text{const}$. Then for the variable Φ we have

$$\dot{\Phi} = -R\mu^{-1} e^{-\alpha t} \sin \Phi.$$

Upon separation of the variables

$$\frac{d\Phi}{\sin \Phi} = -\frac{R}{\mu} e^{-\alpha t}$$

the integration yields

$$\text{tg} \frac{\Phi(t)}{2} = \exp \left[\frac{R(e^{-\alpha t} - 1)}{\mu\alpha} \right] \left(\text{tg} \frac{\Phi(0)}{2} \right).$$

Then we notice

$$\dot{\varphi} = \Omega = R\mu^{-\frac{1}{2}}e^{-\alpha t} \sin \Phi = -\sqrt{\mu}\dot{\Phi},$$

and hence

$$\varphi(t) - \varphi(0) = -\sqrt{\mu}\Phi(t) + \sqrt{\mu}\Phi(0).$$

The relationships we obtain allow us to write down the map, expressing the state vectors $\mathbf{x}_n = (u_n, \Omega_n, \varphi_n)$ in the reduced phase space, referring to the time instants just before the successive kicks:

$$\mathbf{x}_{n+1} = \mathbf{f}(\mathbf{x}_n). \quad (3.2)$$

The explicit formula for the function \mathbf{f} is rather cumbersome. We present it here in a compact formulation convenient for computations. Namely, with $\mathbf{x}_n = (u_n, \Omega_n, \varphi_n)$, we set

$$\bar{\Omega} = \Omega_n + k\mu^{-1} \sin \varphi_n, \quad (3.3)$$

$$\begin{aligned} R^* &= \sqrt{u_n^2 + \mu\bar{\Omega}^2}, & F^* &= \arg(u_n + i\bar{\Omega}\mu^{1/2}), \\ Y^* &= \tan(F^*/2), & f^* &= 2 \arctan Y^*, \end{aligned} \quad (3.4)$$

$$\bar{f} = 2 \arctan \left[Y^* \exp \frac{R^*(e^{-\alpha T} - 1)}{\mu\alpha} \right], \quad (3.5)$$

$$\begin{aligned} u_{n+1} &= R^* e^{-\alpha T} \cos \bar{f}, & \Omega_{n+1} &= R^* e^{-\alpha T} \sin \bar{f}, \\ \varphi_{n+1} &= \varphi_n - (\bar{f} - 2 \arctan Y^*)\mu^{1/2}. \end{aligned} \quad (3.6)$$

In the next section, we turn to the study of the dynamics described by the map derived in terms of types of attractors, which depend on the parameters of the problem. The question of how the motions of the sleigh on a plane relate to these attractors will be discussed in Section 5.

The proposed method of description of motions of the Chaplygin sleigh in discrete time is similar to the discretization method leading to the Chirikov map when considering a mathematical pendulum excited by external kicks [1, 3]. In this case, the system (3.2) should be regarded as the simplest model in the study of kicked nonholonomic systems with weak viscous friction. It is remarkable that the proposed procedure is unique, has a clear physical meaning, and does not have a strong arbitrariness, as is the case in many developed models of discrete nonholonomic systems (a review of them is presented, in particular, in [27]). Our approach can also be compared with a slightly different procedure for obtaining a piecewise linear model of the nonholonomic Chaplygin sleigh proposed by Ruina [12] and investigated qualitatively by Coleman and Holmes [28].

4. ATTRACTORS IN THE REDUCED PHASE SPACE IN DIFFERENT MODES

Figure 2 shows plots of the time dependences for the velocity and the angular velocity of the Chaplygin sleigh in steady motion modes. They are obtained from the results of numerical integration of Eqs. (3.1) at $\mu = 7$, $T = 100$, $\alpha = 0.05$, $\alpha_0 = 0.35$ and indicated on the diagrams for different values of k . The modes in diagrams *a* and *b* are periodic, respectively, with a period of two and four time intervals of the kicks. Diagrams *c* and *d* show no visible repetition of the forms of certain periods and, as we will see, they are actually chaotic.

Figure 3 shows portraits of attractors for different values of the kick intensity parameter k on the plane of the variables (u, Ω) in stroboscopic presentation at time instants immediately after each successive kick.

In diagrams *a*, *b*, *c*, *g* in the Poincaré sections the attractors correspond to finite sets of points and relate to periodic dynamics. The attractors on panels *d*, *e*, *f*, *h* are chaotic.

Figure 4 shows a chart of dynamical regimes of the reduced system. To depict the chart, we scan the parameter plane over the grid with a certain small pitch in two dimensions. Since we assume the relationship between the parameters $\alpha_0 = \mu\alpha$, the map defined by the relations (3.3)–(3.6) accurately describes the dynamics. At each point of the parameter plane grid we perform about 10^3 iterations of the map, and the data for the end subsets of the iterations are analyzed to detect the presence of the repetition period from 1 to 14, with some predetermined low level of permissible

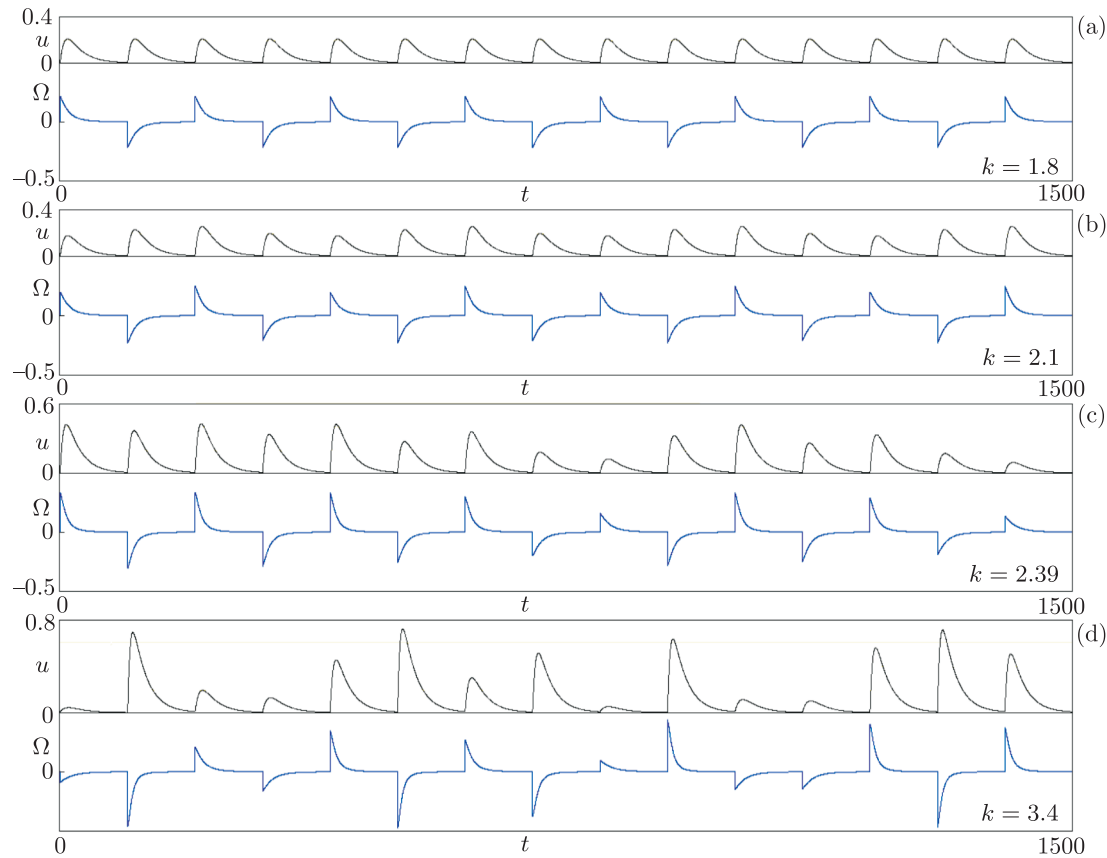


Fig. 2. Dependences of the translation and angular velocities on time in sustained modes of motion of the Chaplygin sleigh plotted according to the results of numerical integration of Eqs. (3.1) at $\mu = 7$, $T = 100$ with the values of k indicated on the diagrams.

error. As the periodicity is detected, we mark the corresponding pixel with a certain color, and the routine proceeds with analyzing the next point in the parameter plane.

The blue area in the bottom part of the chart corresponds to the situation where the attractor is a fixed point, with zero translation and angular velocity, i. e., it corresponds to the non-moving sleigh. Here the rotation angle comes to the fixed value of π as the final result of the temporal evolution.

With further increase of the parameter k a bifurcation occurs with transition to the regime of period $2T$ (dark green area on the chart), which obeys the symmetry $\varphi_{n+1} = \varphi_n$. The next bifurcation is symmetry break, without changing the period, which corresponds to transition to the light green area. Then, on the basis of the arising asymmetric periodic mode a sequence of period-doubling bifurcations follows corresponding to Feigenbaum's transition to chaos.

Figure 5 shows the same area in the parameter plane, where the largest Lyapunov exponent of the stroboscopic map is indicated by gray tones for negative values (regular motions), and by uniform brown color for positive values (chaos). It is productive to compare the charts of Figs. 4 and 5 as mutually complementing distinct forms of visualization of the parameter plane topography.

Figure 6 shows a one-parameter bifurcation diagram ("bifurcation tree") and a plot for three nontrivial Lyapunov exponents depending on the parameter k , which illustrate the transition to chaos through period-doubling bifurcations. The diagrams correspond to the path on the parameter plane chart from bottom up, in the indicated limits of k , with constant $\mu = 7$. The bifurcation tree at the threshold of chaos and plot of the senior Lyapunov exponent have well-recognizable forms characteristic of the period-doubling scenario of transition to chaos through the bifurcation cascade, which obeys the Feigenbaum universality and scaling regularities [1, 3, 32]. This qualitative conclusion is confirmed by numerical estimates for the constant of convergence of bifurcation points to the limit of their accumulation ($\delta \approx 4.7$) and for the constant characterizing the splitting of the tree branches ($\alpha \approx -2.5$).

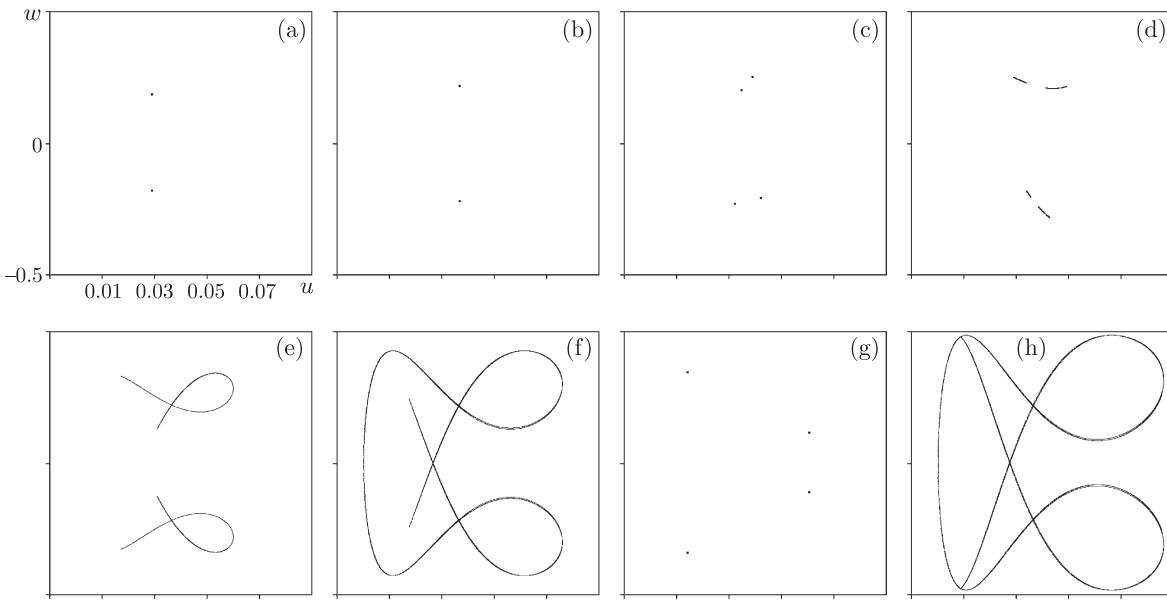


Fig. 3. Portraits of attractors on the plane of variables (u, Ω) corresponding to the stroboscopic cross-section at time instances immediately after each successive pulse propulsion at $T = 100$, $\alpha = 0.05$, $\mu = 7$ and different values of kick intensity parameter $k = 1.3$ (a), 1.8 (b), 2.1 (c), 2.19 (d), 2.39 (e), 3.00 (f), 3.15 (g), 3.4 (h).

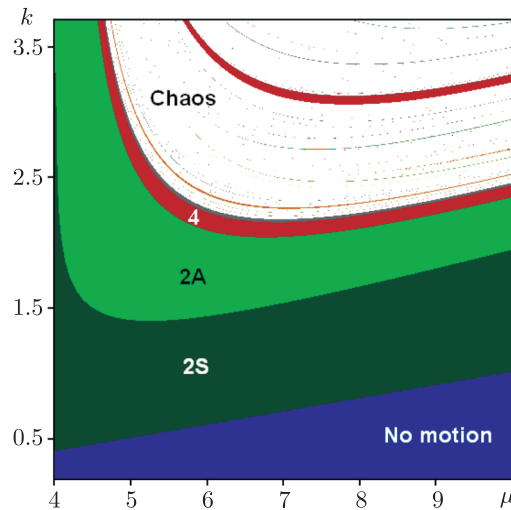


Fig. 4. Chart of dynamics of the Chaplygin sleigh on a plane of parameters μ and k , respectively, the moment of inertia and the intensity of kicks, while the period of pulses is $T = 100$ and the dissipation parameter is $\alpha = 0.05$. The blue color corresponds to the absence of motion of the sleigh. Dark green and light green colors represent, respectively, symmetric (2S) and asymmetric (2A) motions with a period of the velocity variables $2T$, and other colors designate motions with other periods given by multiples of T . White color corresponds to unrecognized periods (actually, the chaotic dynamics).

5. MOVEMENTS OF THE SLEIGH CORRESPONDING TO DIFFERENT TYPES OF ATTRACTORS

To imagine what the real motion of the sleigh on a plane looks like, we note that it is possible to represent it as composed of fragments corresponding to the sequent displacements of the sleigh in time intervals between successive periodic kicks. Figure 7 shows such fragments of the trajectories realized when starting from one and the same point O with zero initial velocity after a kick, depending on the initial orientation of the sleigh. If the repetition period of kicks is large enough, the sleigh nearly stops at the end of the path shown on the picture, and further motion will

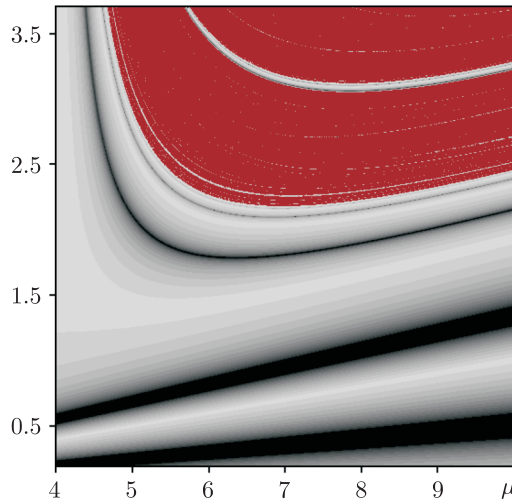


Fig. 5. Lyapunov exponent chart on the parameter plane of μ and k at $T = 100$ and $\alpha = 0.05$. The shades of gray indicate the levels of the senior Lyapunov exponent. The near-zero values correspond to light gray, and the large negative values to dark gray tones. The area of positive Lyapunov exponent corresponding to chaos is uniformly brown in color.

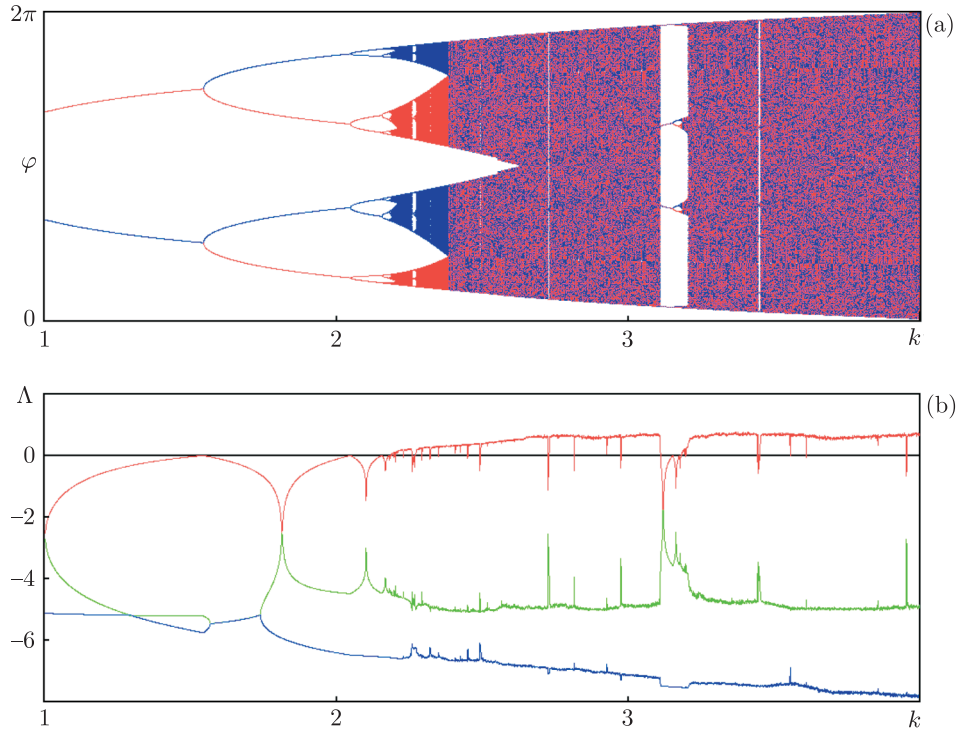


Fig. 6. Bifurcation tree which shows the values of the angular coordinate φ corresponding to instants of the kicks, where the blue and red branches correspond to coexisting distinct attractors (a). The regions where the blue and the red dots are intermixed correspond to the combined response to unified attractors. The plot for three nontrivial Lyapunov exponents (b) depending on the intensity of kicks at $T = 100$, $\alpha = 0.05$, $\mu = 7$.

correspond to a new path fragment from the same set that we should attach, but with respective shift to the position reached, and with the initial angle realized to this instant at that point.

Figure 8 shows a set of trajectories obtained from numerical solution of Eqs. (2.1) with the same parameters, which correspond to the portraits of attractors in the stroboscopic section in Fig. 3. From left to right, the first path corresponds to the symmetric cycle of period 2 of the reduced equations. One can see a repetition over and over again for a certain form over two periods of kicks.

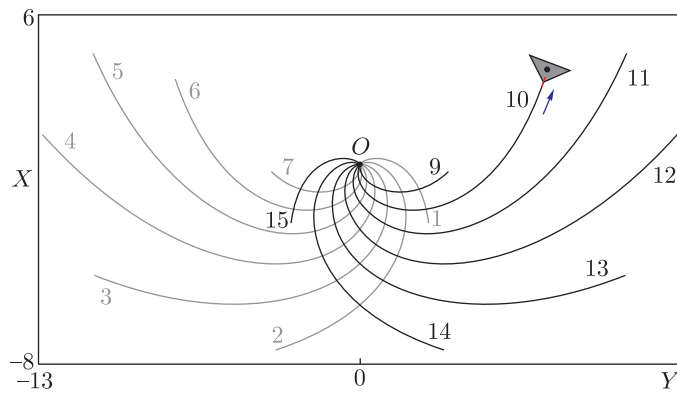


Fig. 7. Trajectories produced by the Chaplygin sleigh in the laboratory frame of reference with the start from point O with zero initial velocity after a kick depending on the initial orientation. The numbers m given at respective trajectories indicate the initial values of the angle $\varphi = \pi m/8$. The parameters are $\alpha = 0.05$, $\mu = 7$, $k = 3$. The orientation of the sleigh is illustrated by the icon at the end of path 10.

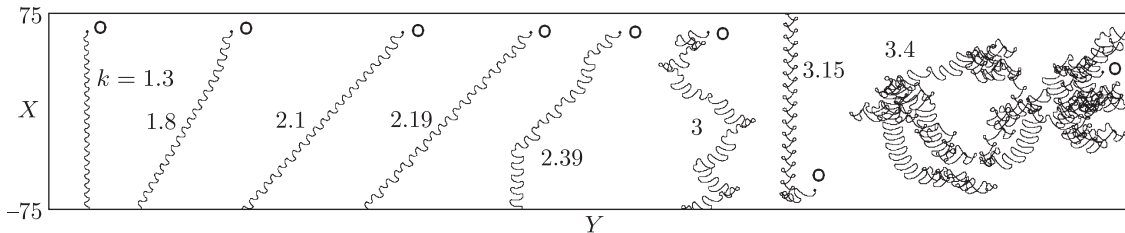


Fig. 8. Examples of the Chaplygin sleigh trajectories in the laboratory frame of reference for different values of the intensity parameter of kicks k . The initial velocity is zero, the initial angle of rotation is $\varphi = \pi/2$. The parameters are $\mu = 7$, $T = 100$, $\alpha = 0.05$, $\alpha_0 = \alpha\mu = 0.35$.

For a symmetric cycle the motion takes place on average along a straight line directed in parallel to the axis X . For an asymmetric cycle the motion takes place along a straight line inclined at some angle θ to the axis X , or, alternatively, at angle $(-\theta)$ depending on initial conditions. Similar patterns are observed in situations of motions with larger periods, up to the transition to chaos. In the chaotic region the path becomes wandering, and along with the directional component a diffusion component appears. The diffusion component becomes dominant at the high intensity of kicks. Under such conditions, of interest may be the possibility of navigating the sleigh using the chaos control technique [23–25].

Figure 9 shows the distance traversed by the sleigh depending on the parameter k for time periods of 500 kicks (panel a) and the azimuth angle of the arrival place of the sleigh (panel b).

As can be seen, the sleigh’s motion generally contains a directed and a random component. To characterize the directed motion, one can use the average velocity

$$\bar{v} = \lim_{n \rightarrow \infty} \frac{\sqrt{x^2(nT) + y^2(nT)}}{n},$$

and for the random component an appropriate quantifier is the diffusion coefficient

$$D = \lim_{n \rightarrow \infty} \frac{x^2(nT) + y^2(nT) - \bar{v}n}{n}.$$

Figure 10 shows the numerically obtained dependence of these quantities on the parameter of intensity of kicks.

6. CONCLUSION

We have considered the dynamics of the Chaplygin sleigh under periodic torque pulses, the magnitude of which depends on the spatial orientation of the sleigh, in the presence of a weak viscous friction.

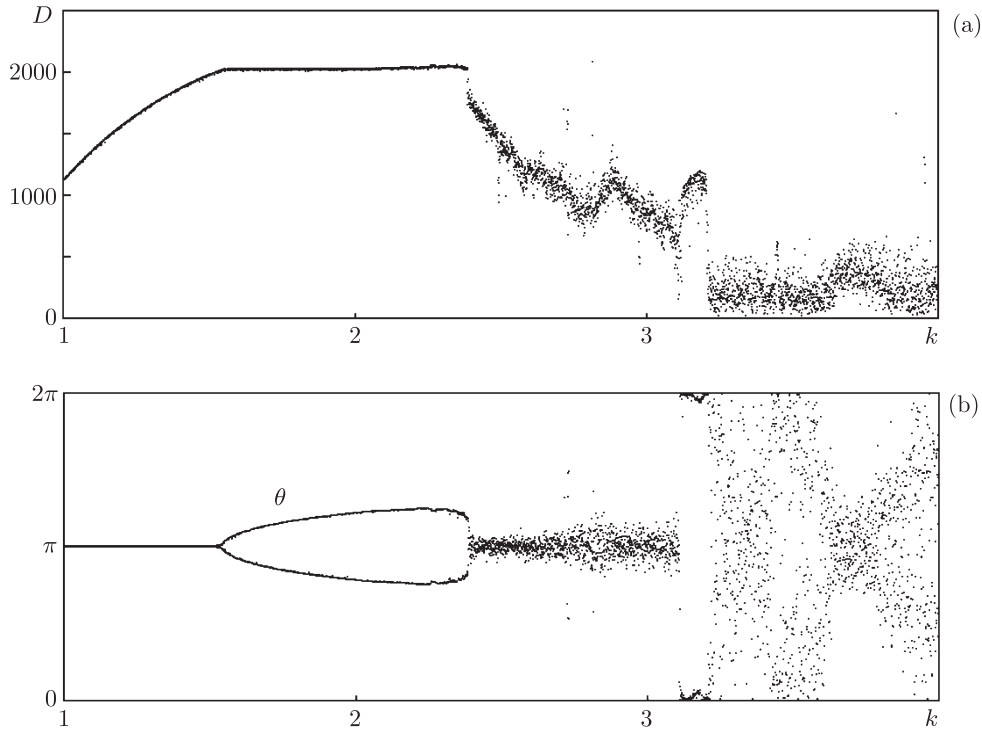


Fig. 9. The distance from the starting point and the azimuth of the point of arrival of the Chaplygin sleigh under t periodic kicks of torque through the time interval of $500T$ after the launch. The parameter values are $\mu = 7$, $T = 100$, $\alpha = 0.05$, $\alpha_0 = \alpha\mu = 0.35$.

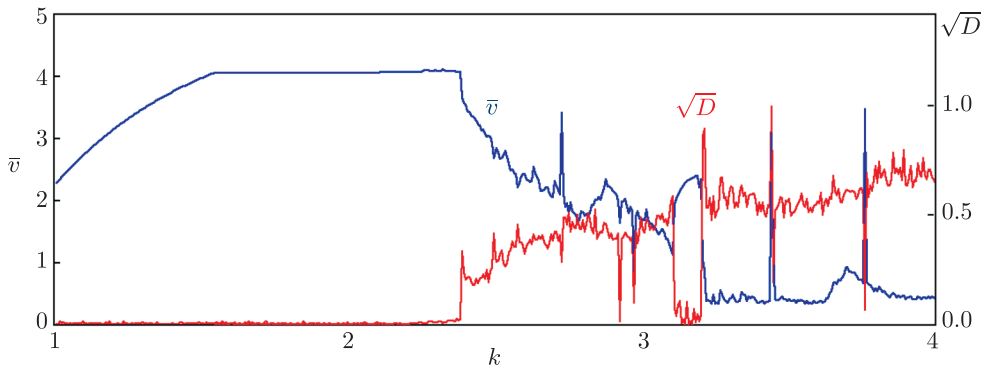


Fig. 10. The dependence of the average velocity of the Chaplygin sleigh and of the diffusion coefficient on the parameter of intensity of kicks. The parameter values are $\mu = 7$, $T = 100$, $\alpha = 0.05$, $\alpha_0 = \alpha\mu = 0.35$.

The occurrence of regular and chaotic motions depending on the intensity of kicks is established. At low intensities the sleigh asymptotically comes to rest at the knife edge orientation in the direction of the external field providing the zero level of the kicks. With increasing intensity of kicks, the mode appears initially with oscillating velocity of period two and with average motion in the direction parallel to the external field. Then, after the symmetry-break bifurcation, the movement takes place at some angle to the field direction (there are two possible directions of motion depending on initial conditions). Further increase in the driving is accompanied by a cascade of period-doubling bifurcations and a Feigenbaum’s transition to chaos.

In weakly chaotic modes, the directional movement dominates, being complemented with slight random-like diffusion component of motion. In situations of developed chaos, the random walk becomes a major contribution to the motion, while the directional movement becomes almost imperceptible. In this situation it is expected that effective may be using chaos control technique in application to the sleigh navigation.

It would be interesting to extend the results obtained to the problem of motion of coupled Chaplygin sleigh systems; this setup also relates directly to wheeled vehicle dynamics problems [29, 30]. Moreover, it would be of interest to consider situations of excitation of nonholonomic systems not with external forces, but using variations in time for internal parameters, just as it has been implemented in a recent example discussed in [31].

ACKNOWLEDGMENTS

This work was supported by the grant of the Russian Science Foundation No 15-12-20035.

REFERENCES

1. Schuster, H. G. and Just, W., *Deterministic Chaos: An Introduction*, Weinheim: Wiley-VCH, 2005.
2. Guckenheimer, J. and Holmes, P., *Nonlinear Oscillations, Dynamical Systems, and Bifurcations of Vector Fields*, Appl. Math. Sci., vol. 42, New York: Springer, 1983.
3. Kuznetsov, S. P., *Dynamical Chaos*, 2nd ed., Moscow: Fizmatlit, 2006 (Russian).
4. *Applications of Chaos and Nonlinear Dynamics in Science and Engineering: Vol. 3*, S. Banerjee, L. Rondoni (Eds.), Understanding Complex Systems, Berlin: Springer, 2013.
5. *Applications of Chaos and Nonlinear Dynamics in Science and Engineering: Vol. 4*, S. Banerjee, L. Rondoni (Eds.), Understanding Complex Systems, Berlin: Springer, 2015.
6. *Applied Nonlinear Dynamics and Chaos of Mechanical Systems with Discontinuities*, M. Wiercigroch, B. de Kraker (Eds.), World Sci. Ser. Nonlinear Sci. Ser. A Monogr. Treatises, vol. 28, River Edge, N.J.: World Sci., 2000.
7. Gantmacher, F. R., *Lectures in Analytical Mechanics*, Moscow: Mir, 1975.
8. Goldstein, H., Poole, Ch. P. Jr., Safko, J. L., *Classical Mechanics*, 3rd ed., Boston, Mass.: Addison-Wesley, 2001.
9. Neimark, Ju. I. and Fufaev, N. A., *Dynamics of Nonholonomic Systems*, Trans. Math. Monogr., vol. 33, Providence, R.I.: AMS, 1972.
10. Borisov, A. V., Mamaev, I. S., and Bizyaev, I. A., Historical and Critical Review of the Development of Nonholonomic Mechanics: The Classical Period, *Regul. Chaotic Dyn.*, 2016, vol. 21, no. 4, pp. 455–476.
11. Borisov, A. V. and Mamaev, I. S., The Rolling Motion of a Rigid Body on a Plane and a Sphere: Hierarchy of Dynamics, *Regul. Chaotic Dyn.*, 2002, vol. 7, no. 2, pp. 177–200.
12. Ruina, A., Nonholonomic Stability Aspects of Piecewise Holonomic Systems, *Rep. Math. Phys.*, 1998, vol. 42, nos. 1–2, pp. 91–100.
13. Borisov, A. V., Mamaev, I. S., and Bizyaev, I. A., The Hierarchy of Dynamics of a Rigid Body Rolling without Slipping and Spinning on a Plane and a Sphere, *Regul. Chaotic Dyn.*, 2013, vol. 18, no. 3, pp. 277–328.
14. Borisov, A. V. and Mamaev, I. S., Strange Attractors in Rattleback Dynamics, *Physics–Uspekhi*, 2003, vol. 46, no. 4, pp. 393–403; see also: *Uspekhi Fiz. Nauk*, 2003, vol. 173, no. 4, pp. 407–418.
15. Borisov, A. V., Kazakov, A. O., and Kuznetsov, S. P., Nonlinear Dynamics of the Rattleback: A Nonholonomic Model, *Physics–Uspekhi*, 2014, vol. 57, no. 5, pp. 453–460; see also: *Uspekhi Fiz. Nauk*, 2014, vol. 184, no. 5, pp. 493–500.
16. Borisov, A. V., Jalnina, A. Yu., Kuznetsov, S. P., Sataev, I. R., and Sedova, J. V., Dynamical Phenomena Occurring due to Phase Volume Compression in Nonholonomic Model of the Rattleback, *Regul. Chaotic Dyn.*, 2012, vol. 17, no. 6, pp. 512–532.
17. Borisov, A. V., Kazakov, A. O., and Sataev, I. R., The Reversal and Chaotic Attractor in the Nonholonomic Model of Chaplygin’s Top, *Regul. Chaotic Dyn.*, 2014, vol. 19, no. 6, pp. 718–733.
18. Chaplygin, S. A., On the Theory of Motion of Nonholonomic Systems. The Reducing-Multiplier Theorem, *Regul. Chaotic Dyn.*, 2008, vol. 13, no. 4, pp. 369–376; see also: *Mat. Sb.*, 1912, vol. 28, no. 2, pp. 303–314.
19. Carathéodory, C., Der Schlitten, *Z. Angew. Math. Mech.*, 1933, vol. 13, no. 2, pp. 71–76.
20. Borisov, A. V. and Mamaev, I. S., The Dynamics of a Chaplygin Sleigh, *J. Appl. Math. Mech.*, 2009, vol. 73, no. 2, pp. 156–161; see also: *Prikl. Mat. Mekh.*, 2009, vol. 73, no. 2, pp. 219–225.
21. Sagdeev, R. Z., Usikov, D. A., and Zaslavsky, G. M., *Nonlinear Physics: From the Pendulum to Turbulence and Chaos*, Chur: Harwood Acad. Publ., 1990.
22. Argyris, J., Faust, G., Haase, M., and Friedrich, R., *An Exploration of Dynamical Systems and Chaos*, 2nd ed., Heidelberg: Springer, 2015.
23. Ott, E., Grebogi, C., and Yorke, J. A., Controlling Chaos, *Phys. Rev. Lett.*, 1990, vol. 64, no. 11, pp. 1196–1199.
24. Pyragas, K., Continuous Control of Chaos by Self-Controlling Feedback, *Phys. Lett. A*, 1992, vol. 170, no. 6, pp. 421–428.

25. Fradkov, A. L., Evans, R. J., and Andrievsky, B. R., Control of Chaos: Methods and Applications in Mechanics, *Philos. Trans. R. Soc. Lond. Ser. A Math. Phys. Eng. Sci.*, 2006, vol. 364, no. 1846, pp. 2279–2307.
26. Jung, P., Marchegiani, G., and Marchesoni, F., Nonholonomic Diffusion of a Stochastic Sled, *Phys. Rev. E*, 2016, vol. 93, no. 1, 012606, 9 pp.
27. Ferraro, S., Jiménez, F., and Martín de Diego, D., New Developments on the Geometric Nonholonomic Integrator, *Nonlinearity*, 2015, vol. 28, no. 4, pp. 871–900.
28. Coleman, M. J. and Holmes, P., Motions and Stability of a Piecewise Holonomic System: The Discrete Chaplygin Sleigh, *Regul. Chaotic Dyn.*, 1999, vol. 4, no. 2, pp. 55–77.
29. Borisov, A. V., Mamaev, I. S., Kilin, A. A., and Bizyaev, I. A., Qualitative Analysis of the Dynamics of a Wheeled Vehicle, *Regul. Chaotic Dyn.*, 2015, vol. 20, no. 6, pp. 739–751.
30. Borisov, A. V., Kilin, A. A., and Mamaev, I. S., On the Hadamard–Hamel Problem and the Dynamics of Wheeled Vehicles, *Regul. Chaotic Dyn.*, 2015, vol. 20, no. 6, pp. 752–766.
31. Karavaev, Yu. L. and Kilin, A. A., The Dynamics and Control of a Spherical Robot with an Internal Omniwheel Platform, *Regul. Chaotic Dyn.*, 2015, vol. 20, no. 2, pp. 134–152.
32. Feigenbaum, M. J., Quantitative Universality for a Class of Nonlinear Transformations, *J. Stat. Phys.*, 1978, vol. 19, no. 1, pp. 25–52.